Steam-Chest Molding of Expanded Polypropylene Foams. 1. DSC Simulation of Bead Foam Processing

ARTICLE *in* INDUSTRIAL & ENGINEERING CHEMISTRY RESEARCH · SEPTEMBER 2010

Impact Factor: 2.59 · DOI: 10.1021/ie101085s

3 AUTHORS:

Wentao Zhai
Chinese Academy of Sciences
62 PUBLICATIONS **978** CITATIONS
SEE PROFILE

Young-Wook Kim
University of Seoul
260 PUBLICATIONS **3,594** CITATIONS
SEE PROFILE

C.B. Park
University of Toronto
541 PUBLICATIONS **7,008** CITATIONS
SEE PROFILE

Steam-Chest Molding of Expanded Polypropylene Foams. 1. DSC Simulation of Bead Foam Processing

Wentao Zhai,[†] Young-Wook Kim,[†,‡] and Chul B. Park*,[†]

Microcellular Plastics Manufacturing Laboratory, Department of Mechanical and Industrial Engineering, University of Toronto, Toronto, Ontario, M5S 3G8, and Department of Materials Science and Engineering, The University of Seoul, 90 Jeonnong-dong, Dongdaemoon-ku, Seoul 130-743, Republic of Korea

To investigate the evolution of melting behavior during the steam-chest molding process of expanded polypropylene (EPP) bead, a differential scanning calorimetry (DSC) test involving fast heating, isothermal treatment, and fast cooling was used to simulate the bead foam processing. The EPP bead foam had two original melting peaks: a low melting peak, T_{mlow}, and a high melting peak, T_{mhigh}. A new melting peak, T_{mi}, was induced in the DSC curves, resulting from the heating process, when the treatment temperature was 80−150 °C. The T_{mi} was about 7 °C higher than the treatment temperature and tended to increase linearly with the increased treatment temperature. A new melting area and further a melting peak, T_{mc}, were observed in DSC curves, resulting from the cooling process, when the treatment temperatures were higher than 135 °C. The high sensitivity of the T_{mi} and T_{mc} to treatment temperature provided a clue to the actual temperature inside the mold during the steam-chest molding process. Different steam pressures were applied during EPP bead processing, and the melting behavior of molded EPP samples was measured to check the processing thermal history. A comparison study was done between the DSC simulations and the actual results to understand the melting behavior evolution of EPP bead foam during processing. Some fundamental issues in the steam-chest molding processing, such as the actual steam temperature, the temperature gradient across the mold cavity, and the accurate pressure parameter used to describe the actual processing temperature were also studied based on the DSC simulation.

Introduction

Expanded polystyrene (EPS), expanded polyethylene (EPE), and expanded polypropylene (EPP) are three kinds of widely used modern moldable bead foams, and they are produced by very different methods.[1,2] Unlike the preparation of EPS beads, EPP beads must be expanded as soon as they are impregnated with a blowing agent due to the blowing agent's high diffusion rate under atmospheric pressure.[3] Consequently, EPP beads have an extremely large volume, which leads to costly transportation. EPP bead foam also has a high melting peak of about 150−170 °C, and high steam temperatures and pressures are required for processing. In addition, EPP products often require post-aging to stabilize cell structure because of the slow crystallization rate of the used polypropylene (PP) resin.[1] These factors all add complexity to the process and make EPP bead foams about three times more expensive than EPS bead foams. Despite these drawbacks, EPP bead foams continue to be one of the fastest growing products used in the automotive industry as well as in transport packaging, because of their capacity to withstand repeated impact and compression.[1,4−8] Since the late 1980s, EPP bead foams entered the automotive field as a core material in bumper impact protection.[4] EPP bead foams have also been moving into more complex applications in such areas as energy management, acoustic preference, and structural support.[1−4,9]

Steam-chest molding is a commercial method used to manufacture molded bead foam products, and its working mechanism is very like a sintering process. The main difference between them is that the former uses high temperature steam as an effective heating/cooling medium,[10,11] while the latter normally uses hot air.[12−14] By utilizing the steam-chest molding machine, a 3-dimensional molded bead foam product with a specific shape can be produced. This provides more opportunity to meet the various product design requirements of applications. During the steam-chest molding process,[15,16] high temperature steam is injected periodically into the mold from two directions to soften and fuse the beads. Meanwhile, the steam can penetrate and condense in the bead foams. When depressurized, the condensed water in the cells begins to gasify and contribute to expansion of the foams together with the expanding air, resulting in the development of fused flat faces at the beads' interface. With the help of the water cooling that follows, the beads' interfaces solidify and efficient bonding is made among the beads foams. In steam-chest molding, the steam pressure is used to adjust the steam temperature.[15] It is generally known that the steam temperature is a critical parameter affecting the mechanical properties of final molded EPP samples, and optimum processing conditions can be reached by trial and error. To our knowledge, however, the evolution of the melting behavior of EPP bead foams during processing and the working mechanism of steam temperature on the interface bonding of beads are still unclear. In addition, during processing the steam pressure keeps changing, and it is difficult to determine the actual temperature in the mold. Furthermore, considering the large volume and complicated shape of the mold cavity, the temperature distribution across the mold cavity is also not clear.

Using a numerical simulation method,[16] Nakai et al. investigated some fundamental aspects of steam-chest molding, such as the evaporation and condensation of steam, and heat conduction. In this study, we used a differential scanning calorimetry (DSC) test to simulate EPP processing with steam-chest molding, where fast heating, isothermal treatment followed by fast cooling was carried out. Two kinds of EPP beads with difficult expansion ratios were used. The effect of the heating

* To whom correspondence should be addressed. E-mail: park@mie.utoronto.ca.
[†] University of Toronto.
[‡] The University of Seoul.

10.1021/ie101085s
Published on Web 09/17/2010

Table 1. Characteristics of EPP Beads

sample	grade	expansion ratio	bulk density (g/L)
EPP15	ARPRO 5446	15 times	60.9
EPP30	ARPRO 5425	30 times	31.3

Table 2. Applied Steam Pressures during EPP Processing

no.	fixed mold pressure/ bar[a]	moving mold pressure/ bar	max. pressure/ bar
1	1.6/2.0	1.8/2.0	2.0
2	2.1/2.5	2.3/2.5	2.5
3	2.6/3.0	2.8/3.0	3.0
4	2.8/4.0	3.0/4.0	3.9

[a] Atmospheric pressure, which is 1 bar lower than absolute pressure.

rate and isothermal treatment temperatures and times were investigated to describe the melting evolution of EPP beads, and to reveal a quantitative relationship between the treatment temperature and the melting behavior of EPP beads. Molded EPP samples were produced using steam-chest molding by changing the steam pressures. Five locations across the molded sample in the thickness direction were used to check the actual processing thermal history during bead processing. By comparing the actual melting behavior of the molded EPP sample with the DSC simulation result of EPP bead foam, it is possible to understand the evolution of the EPP beads' melting behavior during the steam-chest molding process. Moreover, the DSC simulation result could provide reliable information about the temperature distribution across the mold. It could suggest an accurate parameter to describe the actual steam temperature, even though the steam pressure keeps changing during processing. In Part 2 on this topic, in a separate paper, we will explain the mechanism of the interface bonding among EPP beads and the possible parameters to affect the tensile strength of the molded EPP samples based on the results of the DSC simulation.

Experimental Section

Materials. Two kinds of elliptically shaped EPP beads, i.e., ARPRO 5446 and ARPRO 5425, were supplied by JSP (U.S.). The characteristics of the EPP beads studied, such as expansion ratio and bulk density, are shown in Table 1. The EPP beads were coded as EPP15 and EPP30, respectively, according to their expansion ratios.

Steam-Chest Molding Setup and Procedure. Commercially available lab-scale steam-chest molding equipment (DABO Precision, Korea) was used for this study. The dimensions of the mold cavity were 30 cm × 30 cm × 10 cm. The basic steam-chest molding process includes the following: (1) bead filling in the mold cavity; (2) steam injection from the fixed mold; (3) steam injection from the moving mold; (4) steam injection from both sides of the mold; (5) depressurization; (6) water cooling; (7) vacuum for removing remnant water; and (8) mold opening and ejection. The injected steam pressure can be controlled by changing the fixed mold pressure, the moving mold pressure, and the applied steam pressure during EPP processing as shown in Table 2. The unit of steam pressure used in this study is atmospheric pressure in bar, which is 1 bar lower than absolute pressure.

DSC Analysis. The melting peak (T_m) and crystallinity of EPP bead foams and the molded samples were determined by using Q2000 (TA Instruments) calibrated with indium. The degree of crystallinity was calculated from the integration of the DSC melting peaks and by using 290 J/g as the heat of fusion (ΔH_m) of 100% crystallized PP.[17]

In general terms, the steam-chest molding process consists of fast heating, high temperature treatment, followed by fast cooling process. The total time for steam-chest molding processing was about 3 min. DSC tests were used to simulate steam-chest molding with procedure I, as indicated in Figure 1. The samples were heated with a heating rate of 60 °C/min from 20 °C to a high temperature of about 80−165 °C, and then were treated isothermally for different periods of time. When the isothermal treatment time was reached, the samples were cooled to 20 °C again with a cooling rate of 60 °C/min. The heating−isothermal treatment−cooling procedure was scheduled to simulate the actual steam-chest molding process. Afterward, the samples were heated to 200 °C at 10 °C/min to check the previous thermal history, which included the thermal history of fast heating, isothermal treatment, and fast cooling processes.

The thermal history of molded EPP samples was characterized separately using procedure II, where only a temperature ramp process from 20 to 200 °C with a heating rate of 10 °C/min was carried out, unless otherwise indicated. During EPP processing, the thickness of the molded sample was around 10 cm, and the temperature distribution across the molded sample was not clear. The molded EPP samples were cut in the middle, as indicated by dotted lines in Figure 2. Five points with the same distance in thickness direction from one surface to the other were selected to investigate the thermal history.

Results and Discussion

Thermal Behaviors of EPP Beads. During bead processing, the steam penetrates into the interbead void and bead matrix,

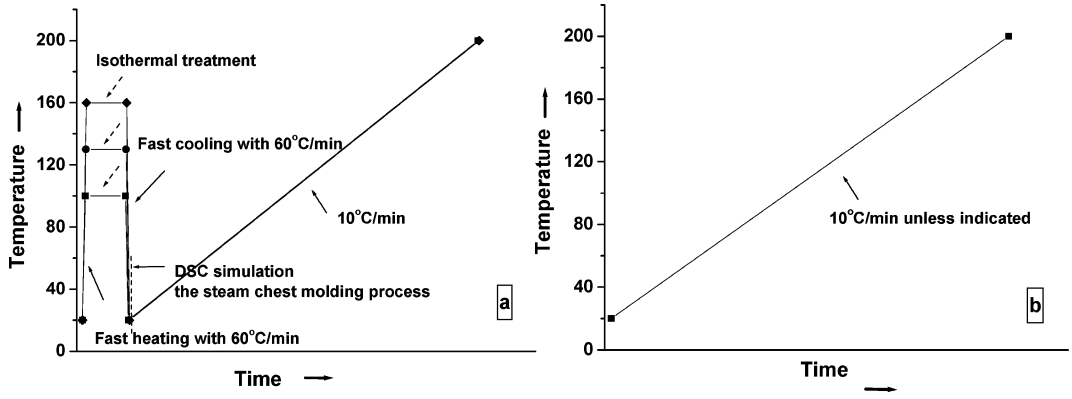

Figure 1. Schematic of DSC tests with procedures I (a) and II (b). In procedure I, the steam-chest molding process was simulated in EPP bead foams, and a temperature ramp with heating rate of 10 °C/min was used to check the thermal history of EPP bead foam during the DSC simulation. In procedure II, a temperature ramp with heating rate of 10 °C/min was used to check the thermal history of the molded EPP sample during steam-chest molding process.

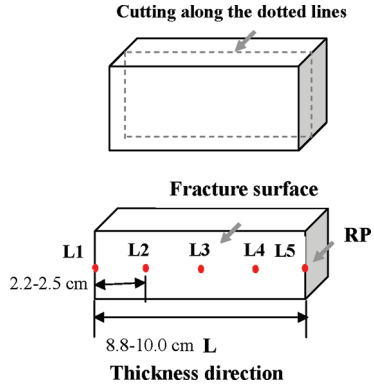

Figure 2. Schematic of specimen preparation for DSC test. Five locations with the same distance in the thickness direction were selected from one surface to the other. The thickness of mold cavity is 10 cm.

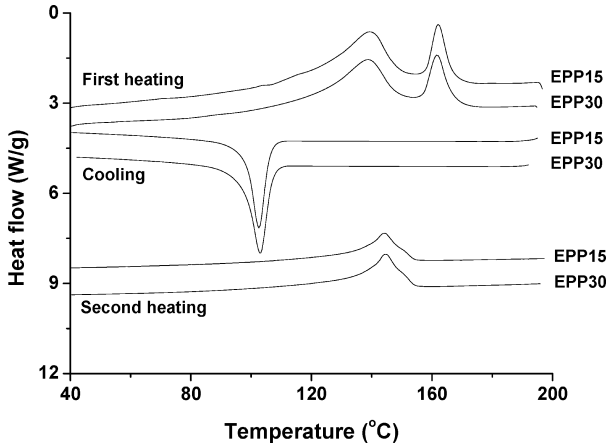

Figure 3. DSC thermograms of EPP15 and EPP30 beads during the heating−cooling−heating process. The heating and cooling rates were 20 °C/min.

working as a heating medium to soften and fuse the beads, and induces bonding between them during the cooling process that follows. In this study, the evolution of EPP beads' melting behaviors was investigated to simulate the steam-chest molding process.

Figure 3 shows the DSC curves of EPP15 and EPP30 beads followed by a heating−cooling−heating process. The bead foams present two melting peaks at 141.2 and 160.9 °C for EPP15, and at 140.9 and 161.1 °C for EPP30 in the first heating curves. In the second heating curves, where the previous thermal history was removed, however, the DSC curves only show a melting peak at 144.1 and 144.5 °C, respectively. These results demonstrate that the double melting peaks of EPP beads presented in the first heating curve stem from the previous thermal history. Moreover, it is seen that the PP resin used for EPP should be a PP copolymer according to its melting peak and crystallization temperature.

Effect of Heating Rate. Figure 4 shows the melting behavior of EPP15 at different heating rates for which procedure II was used. All the DSC curves of the EPP beads exhibit two obvious melting peaks: a sharp high melting peak (T_{mhigh}) and a broad low melting peak (T_{mlow}). As shown, the heating rate had a slight effect on the melting peaks. In the case of the T_{mlow}, it increased from 139.1 to 140.6, 141.4, and 142.5 °C, with a decrease in the heating rate from 40 to 20, 10, and 5 °C/min, respectively, indicating the presence of recrystallization behavior.[18−20] This means that a low heating rate could provide sufficient time to perfect the crystal structures associated with the T_{mlow}. In the case of the T_{mhigh}, however, the temperature increases from 159.2

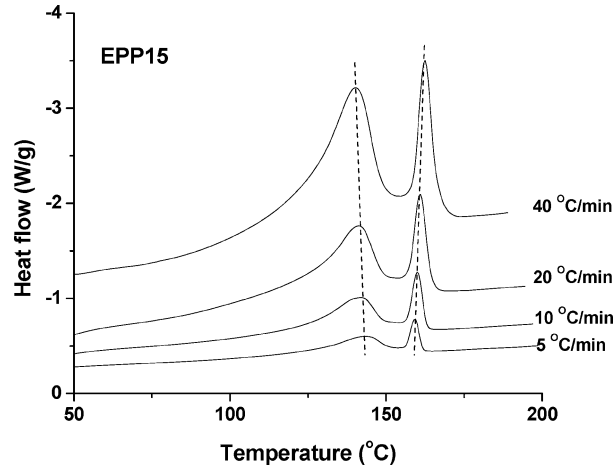

Figure 4. DSC thermograms of EPP15 beads with different heating rates.

to 160.1, 161.3, and 162.5 °C, with heating rate increases from 5 to 10, 20, and 40 °C/min, respectively, suggesting the presence of superheating behavior.[21]

The double melting peaks behavior has been widely observed in iso-PP after isothermal crystallization, which is normally attributed to a difference in crystal lamellar thickness.[22,23] The EPP used in this study was produced by batch foaming, where an annealing process is applied.[24,25] The PP resin contains numerous additives,[2,24,25] and the complexity of its components restricts the study of the origin of double melting peaks in the EPP bead.

Effect of Isothermal Treatment Temperature. Following procedure I, an isothermal treatment was carried out using the DSC test to simulate the steam-chest molding process. Different isothermal treatment temperatures were applied to investigate the evolution of EPP bead melting behaviors.

Figure 5 shows the DSC thermograms of EPP15 and EPP30 beads at different isothermal treatment temperatures. The isothermal treatment time was 3 min, which was similar to the processing time for steam-chest molding. Figure 5a shows that at 80−120 °C the EPP15 bead exhibits two obvious melting peaks, T_{mlow} and T_{mhigh}, which did not change with the isothermal treatment temperature. On the other hand, it is noted that there was a slight melting peak additionally generated at the temperature below the T_{mlow}. This peak was about 7 °C higher than the treatment temperature, and tended to increase linearly with increased treatment temperature. Therefore, it is believed that this new T_{mi} peak was created by the melting of crystals that had possibly been induced by the fast heating and the isothermal treatment that followed. At a treatment temperature of 130 °C, it is interesting to note that the low melting peak at 138.2 °C is differently shaped and little bit lower than the original T_{mlow}. According to the T_{mi} evolution rule with the treatment temperature, it should have been located around 135−137 °C at a treatment temperature of 130 °C. Therefore, this melting peak at 138.2 °C could be the coupling peak of the T_{mi} with the original T_{mlow} at 140.6 °C. At the temperature of 135−145 °C, the original T_{mlow} disappears, and a newly formed T_{mi} appears and its corresponding area decreases with increased treatment temperature. Moreover, a broad melting area was observed, as indicated by the arrow at the temperature lower than the T_{mi}. Corresponding crystals should form during the cooling process, because a high isothermal treatment temperature tends to remove all crystals that should melt at that temperature. At 150 °C, the T_{mi} continues to increase and becomes a shoulder peak of T_{mhigh}.

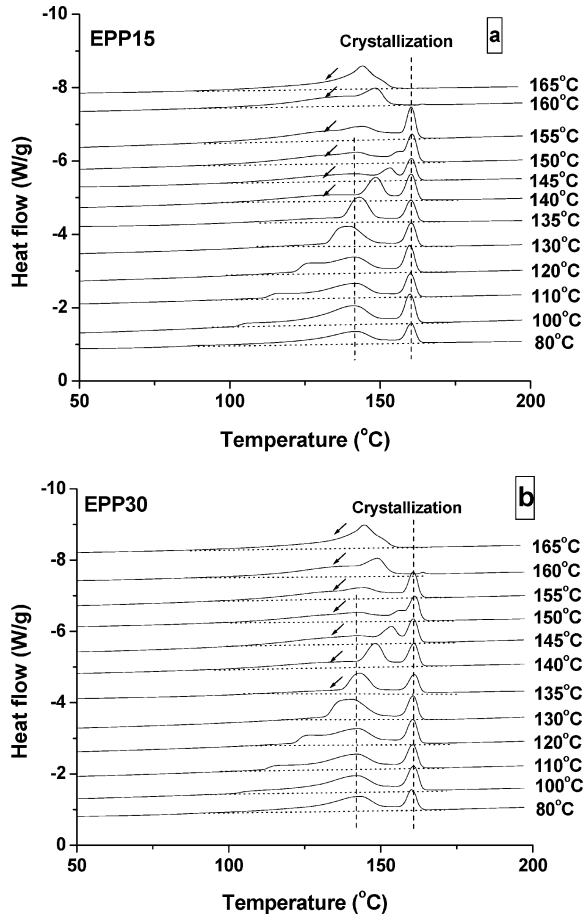

Figure 5. DSC thermograms of EPP15 (a) and EPP30 (b) beads after isothermal treatment at different temperatures.

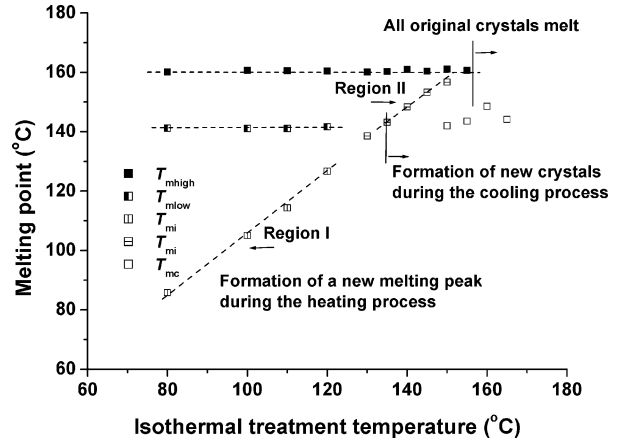

Figure 6. Effect of isothermal treatment temperatures on the melting point of EPP15 beads.

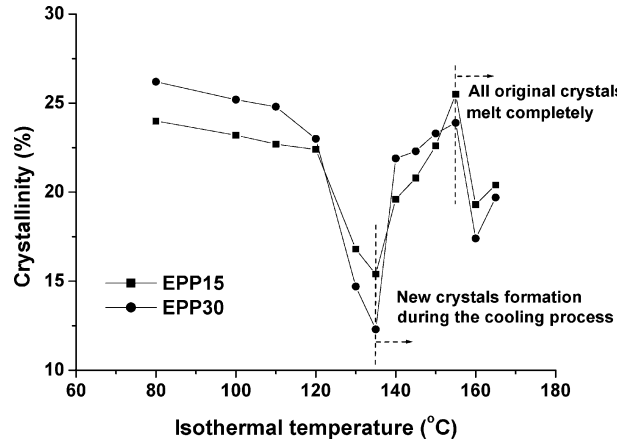

Figure 7. Effect of isothermal treatment temperatures on the crystallinity of EPP15 and EPP30 beads.

On the other hand, there is a new T_{mc} peak at a much low temperature of 141.3 °C, which formed during the cooling process. At 155 °C, the T_{mi} disappears, and the area of the T_{mc} becomes bigger. At this juncture, the T_{mhigh} was still quite stable. At a higher isothermal treatment temperature of 160−165 °C, however, the T_{mhigh} also disappeared, and only a T_{mc} was present in the DSC curve. This phenomenon demonstrated that all original crystals had completely melted, and that the cell structures of the EPP bead foam should be gone. Figure 5b shows the melting behavior of EPP30 bead foam; results very similar to those obtained for EPP15 were observed during isothermal treatment at different temperatures.

For EPP bead foams tested using procedure I, the possible present crystals melting in the DSC curve included the original crystals melting T_{mlow} and T_{mhigh}, which belonged to the EPP bead foam; and the heating-induced (fast heating and isothermal treatment) crystals melting T_{mi} and the cooling-induced crystals melting T_{mc}, both of them belonged to the DSC simulation process. Figure 6 summarizes the melting behavior of EPP15 bead foams at different isothermal treatment temperatures. The EPP30 foams' data are not shown here because of its close similarity to EPP15 data. At a temperature lower than 155 °C the T_{mhigh} was not affected by the treatment temperature, but it was affected when a higher treatment temperature was applied. The T_{mlow} was unchanged at a treatment temperature of no higher than 120 °C, but its corresponding crystallinity tended to decrease gradually with increased treatment temperature. Furthermore, a new T_{mi} melting peak was formed at 80−120 °C (region I). At a treatment temperature of 130−150 °C (region II), the original T_{mlow} disappeared, and was replaced by a new T_{mi}, which exhibited the same slope as in region I. The same slope of T_{mi} with the treatment temperature at both regions I and II provided strong proof of this new peak's origin. Another new melting area was present in the DSC curves of the EPP bead after it was treated at a temperature higher than 135 °C, and a melting peak of T_{mc} was further observed at a treatment temperature higher than 150 °C. It is interesting to note that the T_{mi} was very sensitive and increased linearly with increased treatment temperature. This could offer a guideline for speculation on the steam temperature of a molded EPP sample during the steam-chest molding process.

Figure 7 summarizes the crystallinity of EPP15 and EPP30 beads after treatment at different temperatures. It was found that the crystallinity of EPP15 and EPP30 beads tended to decrease gradually at 80−120 °C, and then to decrease dramatically at 130−135 °C, which was accompanied by the partial melting of the crystals that were associated with the T_{mlow} during the heating process. At a higher treatment temperature of 135−155 °C, the crystallinity of EPP15 and EPP30 beads tended to increase significantly, which was accompanied by the melting of crystals during the heating process and crystallization during the cooling process. Moreover, the increased crystallinity in the cooling process was much higher than the decreased crystallinity in the heating process, resulting in a gradual increase in crystallinity. At 160−165 °C, the crystallinity of EPP15 and EPP30 beads clearly decreased due to the melting of all the original crystals. The crystallinity of samples was formed in the cooling process. It seems that 135 °C was the critical

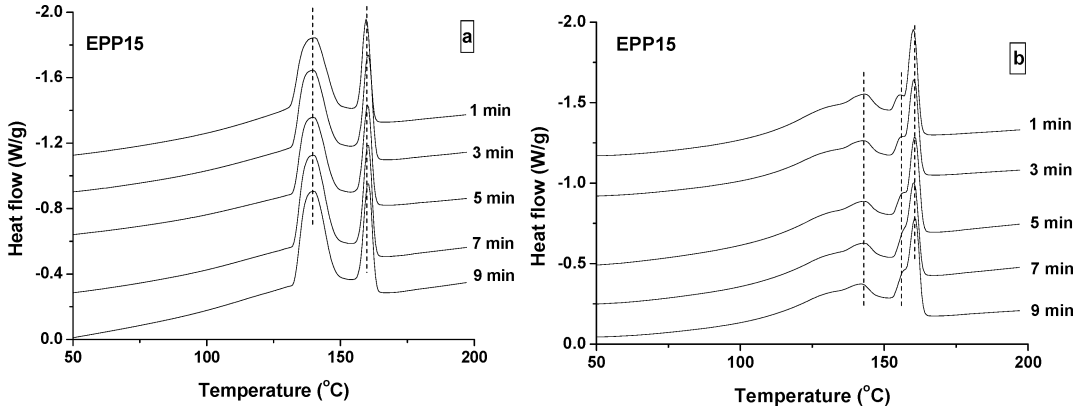

Figure 8. DSC thermograms of EPP15 beads after isothermal treatment at different times at 130 °C (a) and 150 °C (b).

Table 3. Melting Points and Crystallinity of EPP Beads at Different Isothermal Treatment Times

treatment conditions	T_{mi}/T_{mc} (°C)	T_{mhigh} (°C)	crystallinity (%)
130 °C/1 min	138.4/	160.4	16.3
130 °C/3 min	138.2/	160.2	16.7
130 °C/5 min	139.0/	160.4	17.5
130 °C/7 min	138.9/	160.4	18.5
130 °C/9 min	138.5/	160.4	19.0
150 °C/1 min	156.1/141.9	160.2	22.9
150 °C/3 min	156.7/141.7	160.3	22.3
150 °C/5 min	155.6/141.5	160.6	22.1
150 °C/7 min	156.5/141.5	160.2	22.2
150 °C/9 min	157.1/141.1	160.7	21.8

treatment temperature at which EPP15 and EPP30 beads started to crystallize during the DSC simulation process.

Effect of Isothermal Treatment Time. The effect of isothermal treatment time on the thermal behavior of EPP beads was investigated, and the DSC thermograms of EPP15 beads are shown in Figure 8, where the bead foams were isothermally treated at 130 and 150 °C for 1−9 min. At 130 °C, the DSC curve of the EPP15 bead exhibits two peaks: 138.5 and 160.4 °C, which was similar to the melting behavior of the EPP15 bead carried out in procedure II. Furthermore, it seems that the isothermal treatment time did not affect the samples' melting peaks. Similar results were also observed at a high isothermal treatment temperature of 150 °C. These results indicated that EPP beads exhibited quite high thermal stability at a high temperature of 130−150 °C, and a treatment time of 9 min did not damage the cell structure of the foamed EPP beads, which is a significant advantage of the EPP beads used in the steam-chest molding process.

The effect of isothermal treatment time on crystallinity is summarized in Table 3. It is seen that the crystallinity of EPP15 bead foams increases slightly from 16.3% to 16.7%, 17.5%, 18.5%, and 19.0% at 130 °C with increasing treatment time, indicating that more crystals were induced during the treatment process; whereas those for the EPP30 bead foams are 22.9%, 22.3%, 22.1%, 22.2%, and 21.8%, respectively, suggesting that no obvious new crystal regions were induced. As Figure 7 shows, the crystallinity change at 130 °C results mainly from the heating process. A longer heating time might induce more new crystal formations; while those at 150 °C result mainly from the cooling process. However, the increase of isothermal treatment time did not affect the cooling process, and resulted in a nonobvious effect of treatment time on the EPP15 bead's crystallinity.

Thermal Behavior of Molded EPP Samples. During steam-chest molding, the steam pressure that is associated with a specific temperature is an important parameter by which to control the properties of molded EPP samples.[11,26] EPP bead foams were molded by steam-chest molding equipment. Different steam pressures were applied during the processing, as indicated in Table 2, and the attained maximum pressure for each condition was used. In this section, temperature distribution across the mold and the evolution of melting peaks in the molded samples with steam pressure are discussed.

Five locations with the same distance in the molded EPP samples, as indicated in Figure 2, were selected to investigate temperature distribution in the mold during bead foam processing. The real distance between two locations was around 2.2−2.5 cm, which was changing with the experimental conditions because of the shrinkage of molded EPP samples. Figures 9−12 show the DSC thermograms. Table 4 shows the melting behavior and crystallinity of molded EPP15 and EPP30 samples at different steam pressures, where procedure II was used. It can be seen that the melting peaks of the molded EPP samples at different locations are similar no matter what the steam pressures or the size of the bead foams are. Meanwhile, based in Table 4, crystallinity fluctuations at the five locations for each sample in the thickness direction were small. This phenomenon indicated that the thermal history of the EPP beads in the thickness direction were very similar, and further indirectly suggested that the temperature distribution in the mold was quite uniform during the steam-chest molding process. The presence of a negligible temperature gradient from the center to the surface of the mold had been observed in another study,[27] where a formation of interbead channels was required to accelerate the heating and cooling process during the molding cycle.

Another important feature shown in Figures 9−12 and Table 4 is the evolution of EPP beads' melting behaviors during the steam-chest molding process. A temperature ramp using procedure II for those samples was carried out during the DSC tests, which could contain the processing thermal history of EPP beads in the mold. Figure 9 showed that the molded EPP15 and EPP30 samples exhibited two melting peaks: 144.3/160.1 °C and 143.7/160.6 °C, respectively. The low melting peak in the DSC curve was higher than the original T_{mlow} of EPP bead at 140.6 °C, while the high melting peak was almost equal to the T_{mhigh} of EPP bead at 160.4 °C. Based on the results of the DSC simulation, it is believed that the low melting peak should be the T_{mi}, resulting from the heating process during steam-chest molding, and the high melting peak was the original T_{mhigh}, which was not affected by the bead processing. At a steam pressure of 2.5 bar (T_{steam} = 138.9 °C), the low melting peak T_{mi} of molded EPP15 and EPP30 tends to increase from 144.3 and 143.7 °C to 147.7 and 146.9 °C, respectively. This was

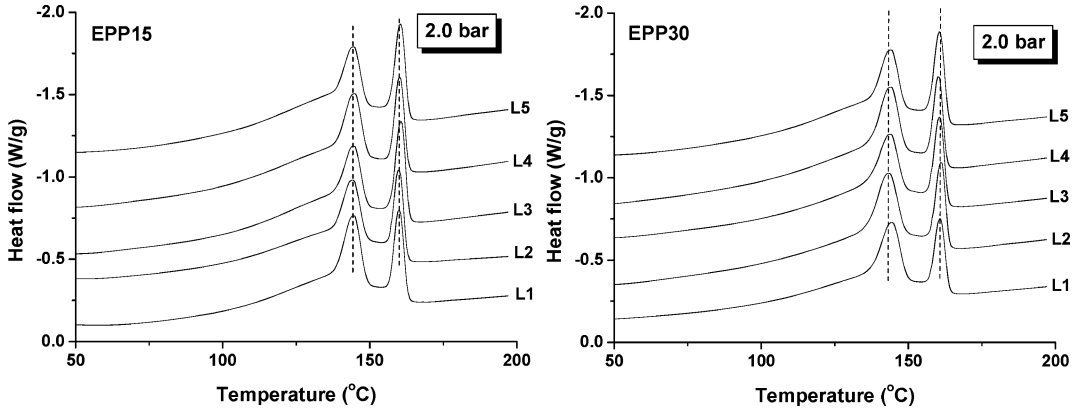

Figure 9. DSC thermograms of molded EPP15 and EPP30 samples with the steam-chest molding process at 2.0 bar atmospheric pressure. L1, L2, L3, L4, and L5 were the 5 locations across the sample in the thickness direction.

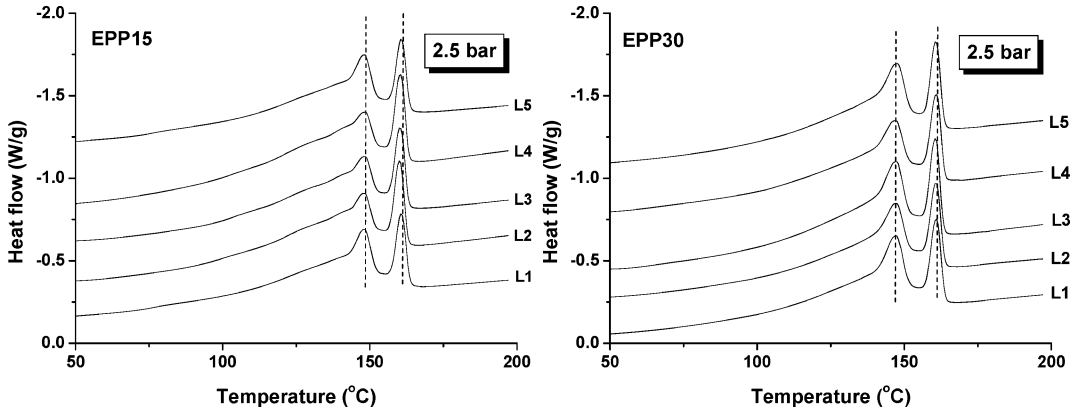

Figure 10. DSC thermograms of molded EPP15 and EPP30 samples with the steam-chest molding process at 2.5 bar atmospheric pressure. L1, L2, L3, L4, and L5 were the 5 locations across the sample in the thickness direction.

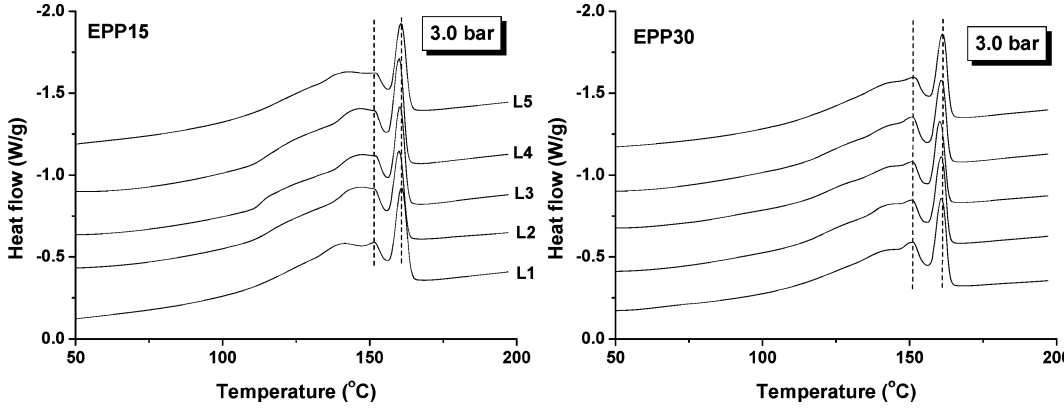

Figure 11. DSC thermograms of molded EPP15 and EPP30 samples with the steam-chest molding process at 3.0 bar atmospheric pressure. L1, L2, L3, L4, and L5 were the 5 locations across the sample in the thickness direction.

very similar to the results of the DSC simulation, where a higher treatment temperature induced a higher T_{mi}. At a steam pressure of 3.0 bar (T_{steam} = 143.6 °C), the T_{mi} of molded EPP15 and EPP30 samples increases gradually to 150.8 and 151.3 °C. Compared with the DSC curve of molded EPP samples at 2.0 (T_{steam} = 133.5 °C) and 2.5 bar, the results obtained at 3.0 bar were very different. Based on the DSC simulation, it seems that the 3.0 bar results were similar to the DSC curve obtained at an isothermal treatment temperature of 145−150 °C, as shown in Figure 5, where the T_{mi} was very high and close to the T_{mhigh}, and a new melting area formed during the cooling process. At a higher steam pressure of 3.9 bar (T_{steam} = 151.9 °C), the T_{mi} tends to disappear or to become very weak at a higher temperature, and a new melting peak, i.e., T_{mc} at 141.4 °C/145.7 and 143.4 °C for the molded EPP15 and EPP30 samples, respectively, was formed during the cooling process. The result at a steam pressure of 3.9 bar was similar to the DSC simulation at 150−155 °C. Therefore, by comparing the DSC results obtained from steam-chest molding with those obtained from the DSC simulation, it is believed that the evolution tendency of T_{mi} and T_{mc} in both cases was quite similar, which demonstrated that the results of the DSC simulation using procedure I was reliable.

Melting Behaviors Indicating the Actual Temperature in the Mold. During the steam-chest molding process, steam pressure is controlled to adjust the properties of molded bead foams. Thermodynamically, the steam pressure is associated with the specific steam temperature. One question is: Can we

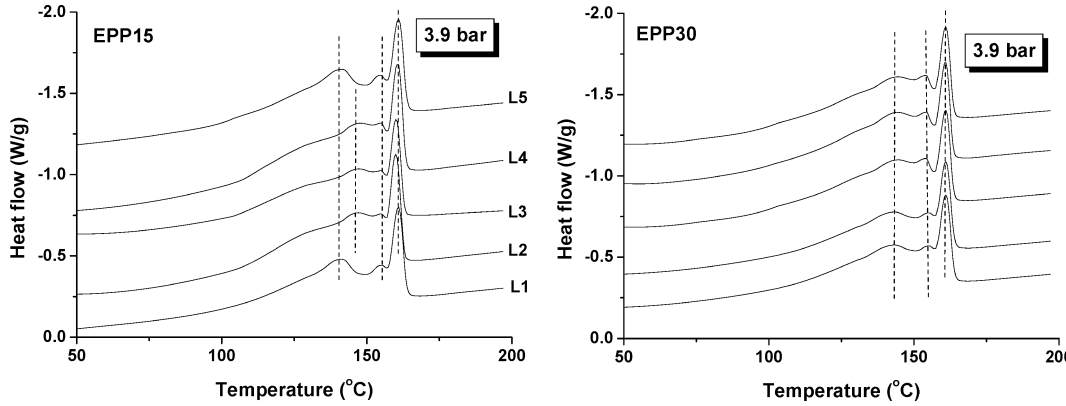

Figure 12. DSC thermograms of molded EPP15 and EPP30 samples with the steam-chest molding process at 3.9 bar atmospheric pressure. L1, L2, L3, L4, and L5 were the 5 locations across the sample in the thickness direction.

Table 4. Melting Points and Crystallinity of Molded EPP Samples at Different Steam Pressures

	EPP15/2.0 bar					EPP30/2.0 bar				
	L1	L2	L3	L4	L5	L1	L2	L3	L4	L5
T_{mi} (°C)	144.6	144.1	144.1	144.6	144.3	144.0	143.9	143.3	143.5	143.6
T_{mhigh} (°C)	159.9	159.8	160.5	160.0	160.3	160.8	161.1	160.6	160.3	160.7
X_c (%)	24.5	25.0	24.9	24.4	24.2	22.4	22.6	23.8	22.9	23.6
	EPP15/2.5 bar					EPP30/2.5 bar				
	L1	L2	L3	L4	L5	L1	L2	L3	L4	L5
T_{mi} (°C)	147.8	147.5	147.7	147.9	147.7	146.8	147.0	146.8	147.1	146.7
T_{mhigh} (°C)	160.2	160.4	160.0	160.2	160.3	160.9	160.7	160.5	160.6	161.0
X_c (%)	22.6	23.0	23.0	23.3	23.1	22.7	22.1	23.2	22.3	22.5
	EPP15/3.0 bar					EPP30/3.0 bar				
	L1	L2	L3	L4	L5	L1	L2	L3	L4	L5
T_{mi} (°C)	151.5	150.8	150.5	150.4	151.7	151.2	151.5	151.4	151.0	151.4
T_{mhigh} (°C)	160.7	159.9	160.3	159.9	160.6	160.9	160.9	160.3	160.7	161.2
X_c (%)	24.6	24.1	23.7	24.6	24.7	22.7	23.2	22.7	22.1	21.8
	EPP15/3.9 bar					EPP30/3.9 bar				
	L1	L2	L3	L4	L5	L1	L2	L3	L4	L5
T_{mc} (°C)	141.3	145.6	146.0	145.8	141.7	143.5	143.2	142.9	143.2	143.7
T_{mhigh} (°C)	160.9	159.9	160.0	160.7	160.9	160.9	160.6	160.9	160.7	161.1
X_c (%)	23.9	25.7	25.2	26.2	24.5	23.1	23.5	24.1	24.2	23.5

know the actual temperature during the steam-chest molding process? Also, considering that the steam pressure keeps changing during bead processing, can we find a pressure parameter to adequately describe each process? To attempt to answer these questions, in this section, we combine the DSC simulation with the actual steam-chest molding process.

Figure 13 shows the evolution of the T_{mi} or T_{mc} of EPP bead foams with the isothermal treatment temperature obtained from the DSC simulation, and those of the molded EPP samples with the steam temperature calculated according to the steam pressure.[28] The maximum pressure in each condition was used. It is observed that the T_{mi} increased linearly with the increased isothermal treatment temperature at 80−150 °C, and the T_{mc} was present at a temperature higher than 150 °C. The steam temperatures at 2.0, 2.5, 3.0, and 3.9 bar atmospheric pressure are 133.5, 138.9, 143.6, and 151.9 °C. The T_{mi} and T_{mc} of molded EPP15 and EPP30 samples at corresponding steam pressures are also shown in Figure 13. It is interesting to note that the three points at steam pressures of 2.0, 2.5, and 3.0 bar were well located along the dotted line of the T_{mi}, and the point at the 3.9 bar was very similar to the T_{mc} at the isothermal treatment temperature of 150 °C, despite the insulating effect of the foam structure of the EPP beads. These results strongly support the reliability of the DSC simulation of the actual steam-chest molding process. Furthermore, the maximum steam pressure of each test could be an accurate parameter by which to describe the actual steam temperature.

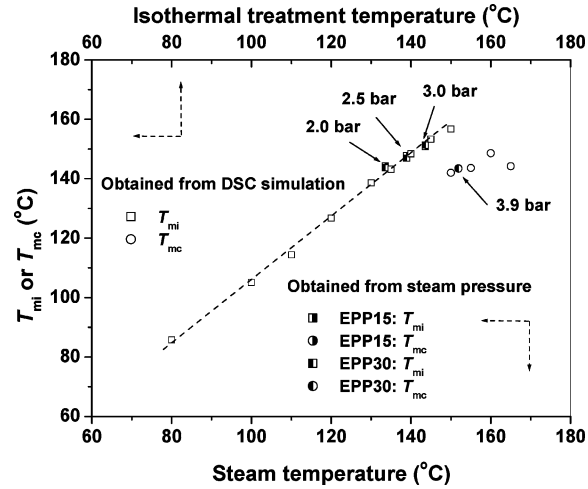

Figure 13. Evolution of the T_{mi} or T_{mc} of EPP bead foams with isothermal treatment obtained from the DSC simulation; and the evolution of the T_{mi} or T_{mc} of molded EPP15 and EPP30 EPP samples with steam temperature obtained from the actual results.

In this paper, DSC simulation was conducted to simulate the steam-chest molding process and verified as an effective way to understand the fundamental issues of EPP processing with steam-chest molding, such as the evolution of the melting behaviors of molded EPP samples, temperature distribution in the mold, and an accurate parameter by which to describe the actual steam temperature. Using DSC simulation results, in the next study (i.e., Part 2 of this study), we focus on the interface bonding of molded EPP samples, and endeavor to understand and explain the parameters that determine the interface bonding between beads.

Conclusions

In this study, a DSC test followed by a fast heating, isothermal treatment, and then a fast cooling process were used to simulate the steam-chest molding process, and the effects of heating rate, different isothermal treatment temperatures and times on the melting behaviors of EPP were carried out. EPP bead foam had two original melting peaks: a low melting peak, T_{mlow}, and a high melting peak, T_{mhigh}. When the isothermal treatment was applied, a new T_{mi} melting peak was induced in the DSC curves. This resulted from the heating process (fast heating followed by isothermal treatment) during the DSC simulation, which was about 7 °C higher than the treatment temperature and tended to increase linearly with the increased treatment temperature at 80−150 °C. A new melting area and then the obvious presence of a T_{mc} melting peak were observed in the DSC curves at 141−146 °C. This resulted from the cooling process during the DSC simulation, when the treatment temperatures were higher than 135 °C. The acute sensitivity of T_{mi} and T_{mc} to the treatment temperature provided an opportunity to anticipate the actual temperature during steam-chest molding.

Different steam pressures were used during EPP bead processing, and the melting behavior of molded EPP samples was measured to check the processing thermal history. By comparing the DSC simulation results of EPP beads and the actual melting behavior of molded EPP samples, it was found that the DSC curves of EPP matched very well in both situations at the same temperature, once the maximum steam pressure in each test was used. This phenomenon suggested that the maximum steam pressure for each test was an accurate parameter by which to describe the actual processing temperature, even though the steam pressure kept changing during the steam-chest molding process. Five locations across the molded EPP sample in the thickness direction were used to investigate temperature distribution in the mold during processing. It was observed that the melting behavior of molded EPP samples was very similar at different locations. These results indicate that the thermal history at those locations was quite uniform during bead processing, suggesting a uniform temperature distribution in the mold cavity.

Acknowledgment

We acknowledge financial support from Consortium of Cellular and Micro-Cellular Plastics (CCMCP) and Korea Research Foundation Grant (KRF-2009-013-D00050).

Literature Cited

(1) Britton, R. *Update on Mouldable Particle Foam Technology*; Rapra Technology: Shawbury, Shrewsbury, UK, 2009.

(2) Eaves, D. *Handbook of Polymer Foams*; Rapra Technology: Shawbury, Shrewsbury, UK, 2004.

(3) Zhang, X.; Zhu, Z.; Park, C. B.; Lee, E. K.; Chen, N.; Naguib, H. E. Study on the Sorption and Desorption of N-Pentane in Polystyrene and Polypropylene. *SPE ANTEC Tech. Papers* **2007**, 3057–3061.

(4) Sopher, S. R. Advanced Development of Molded Expanded Polypropylene and Polyethylene Bead Foam Technology for Energy Absorption. *SPE ANTEC Tech. Papers* **2005**, 2577–2581.

(5) Bureau, M. N.; Champagne, M. F.; Gendron, R. Impact-Compression-Morphology Relationship in Polyolefin Foams. *J. Cell. Plast.* **2005**, *41*, 73–85.

(6) Beverte, I. Deformation of Polypropylene Foam Neopolen®P in Compression. *J. Cell. Plast.* **2004**, *40*, 191–204.

(7) Bouix, R.; Viot, P.; Lataillade, J. L. Polypropylene Foam Behavior under Dynamic Loading: Strain Rate, Density and Microstructure Effects. *Int. J. Impact Eng.* **2009**, *36*, 329–342.

(8) Viot, P. Hydrostatic Compression on Propylene Foam. *Int. J. Impact Eng.* **2009**, *36*, 975–989.

(9) Schut, J. H. Expandable Bead Molding Goes High-Tech. *Plastics Technol.* **2005**, *51*, 68.

(10) Svec, P.; Rosik, L.; Horak, Z.; Vecerka, F. *Styrene Based Plastics and Their Modification*; Ellis Horwood: London, 1990.

(11) Rossacci, J.; Shivkumar, S. Bead Fusion in Polystyrene Foams. *J. Mater. Sci.* **2003**, *38*, 201–206.

(12) Pop-Iliev, R.; Rizvi, G. M.; Park, C. B. The Importance of Timely Polymer Sintering While Processing Polypropylene Foams. *Polym. Eng. Sci.* **2003**, *43*, 40–54.

(13) Pop-Iliev, R.; Lee, K. H.; Park, C. B. Manufacture of Integral Skin PP Foam Composites in Rotational Molding. *J. Cell. Plast.* **2006**, *42*, 139–152.

(14) Bellehumeur, C. T.; Tiang, J. S. Simulation of Non-Isothermal Melt Densification of Polyethylene in Rotational Molding. *Polym. Eng. Sci.* **2002**, *42*, 215–229.

(15) Mills, N. J. *Polymer Foams Handbook: Engineering and Biomechanics Applications and Design Guide*; Butterworth Heinemann: Oxford, 2007.

(16) Nakai, S.; Taki, K.; Tsujimura, I.; Oshima, M. Numerical Simulation of a Polypropylene Foam Bead Expansion Process. *Polym. Eng. Sci.* **2008**, *48*, 107–115.

(17) Wunderlich, B. *Macromolecular Physics, Vol. 1, Crystal Structure, Morphology, Defects*; Academic Press: NewYork, 1973.

(18) Kim, Y. C.; Ahn, W.; Kim, C. Y. A Study on Multiple Melting of Isotatic Polypropylene. *Polym. Eng. Sci.* **1997**, *37*, 1003–1011.

(19) Choi, J. B.; Chung, M. J.; Yoon, J. S. Formation of Double Melting peak of Poly(propylene-co-ethylene-co-1-butene) during the Preexpansion Process for Production of Expanded Polypropylene. *Ind. Eng. Chem. Res.* **2005**, *44*, 2776–2780.

(20) Ren, Z.; Shanks, R. A.; Rook, T. J. Crystallization and Melting of Highly Filled Polypropylene Composites Prepared with Surface-Treated Fillers. *J. Appl. Polym. Sci.* **2001**, *79*, 1942–1948.

(21) Yadav, Y. S.; Jain, P. C. Melting Behavior of Isotactic Polypropylene Isothermally Crystallized from the Melt. *Polymer* **1986**, *27*, 721–727.

(22) Jamomak, J. J.; Cheng, S. Z. D. Isotacticity Effect on Crystallization and Melting in Polypropylene Fractions: 1. Crystalline Structure and Thermodynamic Property Changes. *Polymer* **1991**, *32*, 648–655.

(23) Weng, J.; Olley, R. H.; Bassett, D. C.; Jääskeläinen, P. Changes in the Melting Behavior with the Radial Distance in Isotactic Polypropylene Spherulites. *J. Polym. Sci., Polym. Phys.* **2003**, *41*, 2342–2354.

(24) Tokoro, H.; Kazuo, T.; Utsunomiya, T.; Utsunomiya, H. S.; Utsunomiya, M. O. Uncrosslinked Polyethylene Particles for the Production of Expanded Particles and Uncrosslinked Polyethylene Expanded Particles. U.S. Patent 5459169, 1995.

(25) Tomioka, S. Y.; Hatano, H. K. Process for Producing Prefoamed Polymer Particles. U.S. Patent 4464484, 1984.

(26) Sands, M. MS thesis, Worcester Polytechnic Institute, Worcester, MA, 1998.

(27) Skinner, S. J.; Baxter, S.; Eagleton, S. D. How Polystyrene Foam Expands. *Plast. Eng.* **1965**, *42*, 171–176.

(28) Obtained from http://www.engineeringtoolbox.com/saturated-steam-properties-d_457.html.

Received for review May 12, 2010
Revised manuscript received August 20, 2010
Accepted September 1, 2010

IE101085S